Conformational changes of the H^+-ATPase from *Escherichia coli* upon nucleotide binding detected by single molecule fluorescence

Michael Börsch[a,*], Paola Turina[b], Christian Eggeling[c], Joachim R. Fries[c], Claus A.M. Seidel[c], Andreas Labahn[a], Peter Gräber[a]

[a] *Institut für Physikalische Chemie, Universität Freiburg, Albertstr. 23a, D-79104 Freiburg, Germany*
[b] *Dipartimento di Biologia, Università degli Studi di Bologna, Via Irnerio 42, I-40126 Bologna, Italy*
[c] *MPI für Biophysikalische Chemie, Am Fassberg 11, D-37077 Göttingen, Germany*

Received 1 September 1998

Abstract Using a confocal fluorescence microscope with an avalanche photodiode as detector, we studied the fluorescence of the tetramethylrhodamine labeled F_1 part of the H^+-ATPase from *Escherichia coli*, EF_1, carrying the γT106-C mutation [Aggeler, J.A. and Capaldi, R.A. (1992) J. Biol. Chem. 267, 21355–21359] in aqueous solution upon excitation with a mode-locked argon ion laser at 528 nm. The diffusion of the labeled EF_1 through the confocal volume gives rise to photon bursts, which were analyzed with fluorescence correlation spectroscopy, resulting in a diffusion coefficient of 3.3×10^{-7} cm^2 s^{-1}. In the presence of nucleotides the diffusion coefficient increases by about 15%. This effect indicates a change of the shape and/or the volume of the enzyme upon binding of nucleotides, i.e. fluorescence correlation spectroscopy with single EF_1 molecules allows the detection of conformational changes.

Key words: H^+-ATPase; Conformational change; Fluorescence; Single molecule spectroscopy

1. Introduction

F_0F_1-ATP synthases occur in bacteria, mitochondria and chloroplasts [1]. These enzymes catalyze ATP synthesis coupled with a transmembrane proton flux. They have two large domains: a membrane integrated F_0 part, which is involved in proton transport, and a hydrophilic F_1 part, which contains the nucleotide binding sites. In *Escherichia coli*, the F_1 part contains five different subunits with the stoichiometry $\alpha_3\beta_3\gamma\delta\varepsilon$. Based on functional studies, it was suggested that the catalytic nucleotide binding sites on the β-subunits operate in a cyclic way, which is accomplished by subsequent 'docking-undocking' steps of the γ-subunit to the three αβ pairs. The nucleotide binding and dissociation steps at the F_1 part are coupled in the holoenzyme via long range conformational changes with proton binding, translocation and dissociation steps in the F_0 part (for review see [2]). In this work we investigated conformational changes of the F_1 part of the ATP synthase from *E. coli*, EF_1, which occur upon binding and dissociation of nucleotides. We labeled a cysteine in the γ-subunit of EF_1 with tetramethylrhodamine and measured the fluorescence of single molecules by confocal laser spectroscopy [3]. From an analysis of the fluorescence bursts using fluorescence correlation spectroscopy (FCS), the characteristic time of diffusion of the enzyme through the confocal volume can be derived. We found that the diffusion time changes upon nucleotide binding and conclude that this reflects structural changes in EF_1. A preliminary report of this work has been presented before [4].

2. Materials and methods

Strain pRA114/AN888, carrying the γT106-C mutation, is described in Aggeler and Capaldi [5] and was a gift from these authors. EF_1 was isolated from the mutant strain as described [6] except that the ion-exchange chromatography was performed on a HQ 20 FPLC column (PerSeptive). Isolated EF_1 was stored in liquid nitrogen until use.

The γ-subunit of EF_1 was selectively labeled with substoichiometric amounts of tetramethylrhodamine-5-iodoacetamide (TMRIA, Molecular Probes) in 50 mM MOPS/HCl (pH 7.0) with 10% glycerol as described [7]. EF_1 concentrations were determined by UV absorption using an extinction coefficient of 190 730 M^{-1} cm^{-1} at 280 nm as described [8]. Dye concentrations were determined using an extinction coefficient of 87 000 M^{-1} cm^{-1} at 543 nm. Unbound dye was removed after 4 min reaction time by passing twice through Sephadex G50 centrifuge columns. The labeling of the γ-subunit was specific as determined by the fluorescence of the gel after sodium dodecylsulfate polyacrylamide gel electrophoresis. The TMR labeled enzymes, TMR-EF_1, were stored at −80°C.

Fluorescence measurements were done in 50 mM HEPES/NaOH (pH 8.0) and 2.5 mM $MgCl_2$ (buffer B) after removing fluorescent impurities by activated charcoal granular (1.5 mm, Merck). TMR-EF_1 aliquots were diluted to final concentrations of 10^{-10} M. ATP and β,γ-imidoadenosine-5′-triphosphate (AMPPNP) stock solutions (10 mM) were prepared fresh in buffer B and were mixed with the diluted TMR-EF_1 solutions immediately before the fluorescence measurements. TMR-glutathione was prepared by mixing TMRIA with a 100-fold excess of the tripeptide glutathione (γ-Glu-Cys-Gly, Sigma) and diluted to a final dye concentration of 7×10^{-11} M for single molecule spectroscopy. Confocal fluorescence detection was performed with an active mode locked argon ion laser (excitation wavelength 528 nm, repetition rate 73 MHz) (Sabre, Coherent, Palo Alto, CA) using an epi-illuminated confocal fluorescence microscope (Fig. 1) similar to that described previously [9,10] with a beam-splitter at 530 nm, a 150 μm pinhole and a dichroic band-pass emission filter 582/50 nm (AF Analysentechnik, Tübingen, Germany). The expanded laser beam was attenuated to 530 μW and focused by a water immersion objective (UPLANAPO 60×, NA = 1.2, Olympus) to an excitation volume of a few femtoliters. The fluorescence signal was detected by a single photon counting avalanche photodiode (AQ 151, EG&G, Vaudreuil, Quebec, Canada). The multiplexed detector signal was registered in parallel by a multichannel scaler (MCS) using a PC-adapter counter (CIO-CTR05, Plug-in GmbH, Eichenau, Germany) and by a real-time correlator card (ALV-5000/E, ALV, Langen, Germany) for FCS. The laser focus and detection volume parameters (radial and axial $1/e^2$ radius $\omega_0 = 0.65$ μm and $z_0 = 3.3$ μm, respectively) were determined from FCS measurements of rhodamine 6G

*Corresponding author. Fax: (49) (761) 203-6189.
E-mail: boersch@ruf.uni-freiburg.de

Abbreviations: EF_1, hydrophilic F_1 part of the proton translocating H^+-ATPase from *Escherichia coli*; AMPPNP, β,γ-imidoadenosine-5′-triphosphate; TMRIA, tetramethylrhodamine-5-iodoacetamide; MOPS, 3-[*N*-morpholino] propanesulfonic acid; HEPES, *N*-[2-hydroxyethyl] piperazine *N*′-[2-ethanesulfonic acid]; TMR, tetramethylrhodamine; MCS, multichannel scaler; FCS, fluorescence correlation spectroscopy

PII: S0014-5793(98)01247-2

in pure water with a characteristic diffusion time of $t_D = 0.38$ ms (see Table 1), assuming a translational diffusion coefficient of $D = 2.8 \times 10^{-6}$ cm^2 s^{-1} in water [11]. This corresponds to a detection volume of $V = \pi^{1.5}\ \omega_0^2\ z_0 = 7.7$ fl and a focal area of $A = \pi/2\ \omega_0^2 = 6.7 \times 10^{-9}$ cm^2 [12,13]. Thus, the excitation power of $P = 530$ μW is equivalent to a quasi-continuous focal irradiance of $I_0 = P/A = 8 \times 10^4$ W/cm^2 (see Fig. 1).

The samples were transferred to the microscope support by a microscope slide with a small depression and covered with a conventional cover glass. All measurements were performed at room temperature.

3. Results and discussion

Upon free diffusion in the solution, the TMR-labeled EF_1 enters the confocal detection volume, where the dye is excited by the pulsed laser light and due to the high laser repetition rate cycles continuously between the ground and excited states (see Fig. 1). Fluorescence photons are emitted as bursts when a single enzyme diffuses through the confocal volume. At the mean excitation irradiance of $I_0/2 = 4 \times 10^4$ W/cm^2, the mean number of photons emitted by a single TMR fluorophore in water is about 10^6 before photobleaching occurs [14]. Since the transit time of the labeled EF_1 is about 3 ms, the molecule can emit about 30 000 photons during this period [14]. Assuming a detection efficiency of about 3% [15], about 900 fluorescence photons should be detected from a single molecule transit. Furthermore, the arrangement of the avalanche photodiode with a 150 μm pinhole allows the selective detection

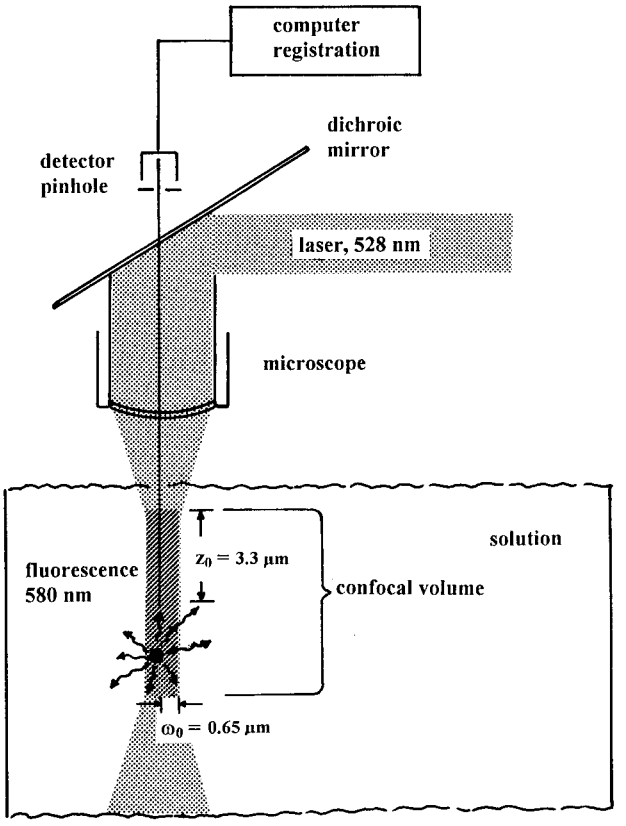

Fig. 1. Scheme of experimental setup for single molecule fluorescence detection. The pulsed laser beam (wavelength 528 nm) is focused through the microscope objective onto the sample. The fluorescence of the sample molecules entering the confocal detection volume is focused on a 150 μm pinhole and detected by a single photon counting avalanche photodiode.

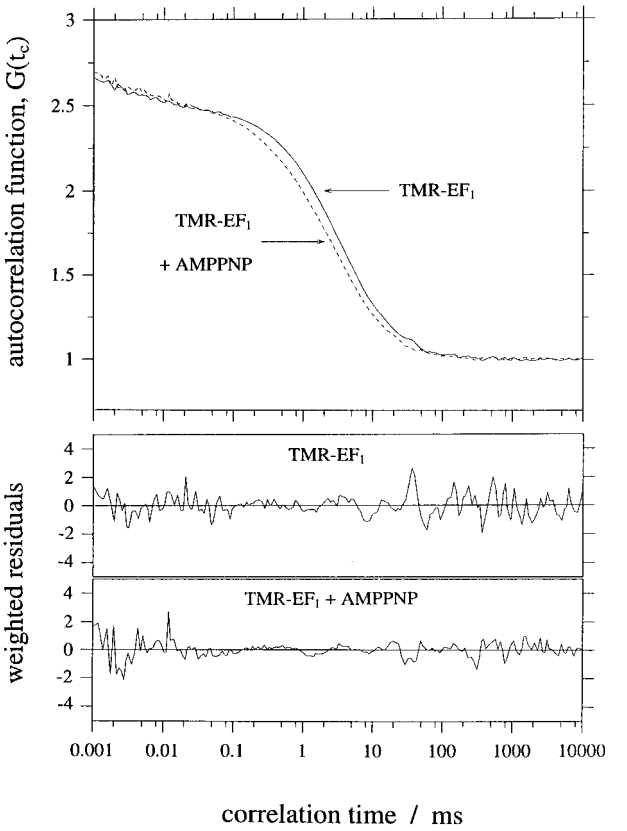

Fig. 2. Multichannel scaler trace of fluorescence signals from EF_1 labeled with tetramethylrhodamine. TMR-EF_1 was diluted in 50 mM HEPES/HCl (pH 8), 2.5 mM $MgCl_2$ to a concentration of 10^{-10} M. Data acquisition was performed at a speed of 1000 points per second (integration time 1 ms). The inset shows an expanded view of two fluorescence bursts.

of the fluorescence from the confocal volume with a strong suppression of background fluorescence from other parts of the solution (see Fig. 1).

Fig. 2 shows a MCS trace of TMR-EF_1 (10^{-10} M in buffer B) to monitor the fluorescence signals (bursts) arising from single TMR-EF_1 molecules diffusing through the confocal detection volume. The single bars of the MCS trace represent the number of fluorescence photons counted by the avalanche photodiode during an integration time of 1 ms. The trace shows burst rates of up to 220 kHz, while a background level of approximately 3 kHz is observed. This corresponds to a signal-to-noise ratio of 70. The background signal mainly results from scattered light and partially from background fluorescence of molecules outside the confocal detection volume. Due to the spatially dependent laser excitation irradiance and fluorescence collection efficiency of the open detection volume, the randomly diffusing molecules can either cross near the edges or traverse the center of the volume. Therefore, an inhomogeneous distribution of the number of detected fluorescence photons from a single molecule transit (burst size) is obtained [15]. This can be seen in Fig. 2, where events of different duration and with different count rates can be seen. The inset in Fig. 2 shows a magnification of a part of the MCS trace, showing a molecule diffusing through the center of the confocal detection volume (burst at 125 ms), and one diffusing through the edge (burst at 110 ms), where the excitation irradiance and, thus, the count rate is smaller.

Table 1
Results of the fluorescence correlation spectroscopy data analysis

Compound	t_T (μs)	T	t_D (ms)	t_A (ms)	A	N_F
Rhodamine 6G	2.1	0.13	0.38	none	none	5.10
TMR-glutathione	2.9	0.06	0.40	none	none	0.26
TMR-EF_1	5.7	0.10	3.2	0.16	0.03	0.60
TMR-EF_1+ATP	5.0	0.11	2.6	0.11	0.05	0.37
TMR-EF_1+AMPPNP	4.4	0.10	2.8	0.20	0.10	0.37

Parameters of a fit of the FCS data to Eq. 1: characteristic triplet correlation time, t_T; average fraction of molecules in the excited triplet state, T; characteristic time for translational diffusion, t_D; average number of fluorescing molecules in the confocal detection volume, N_F; characteristic correlation time of the 'dynamic quenched' state, t_A; and fraction of molecules in the 'dynamic quenched' state, A. The optical parameter (ω_0/z_0) was determined by fitting the FCS data of rhodamine 6G and fixed for all subsequent fits. All other parameters were allowed to vary freely. The estimated error for t_D is 7%.

FCS [12,13] was used to provide precise statistical data on the number of molecules in the detection volume and on the average diffusion time of the molecules through the detection volume. Analysis of the FCS data was performed with a least-squares fit algorithm using the following expression of the normalized autocorrelation function, $G(t_c)$, with the correlation time t_c.

$$G(t_c) = 1 + \frac{1}{N_F}\left(\frac{1}{1+t_c/t_D}\right)\left(\frac{1}{1+(\omega_0/z_0)^2 t_c/t_D}\right)^{1/2} \times (1 - T + T\exp(-t_c/t_T)A + A\exp(-t_c/t_A)) \quad (1)$$

N_F is the average number of fluorescent molecules in the Gaussian detection volume with the $1/e^2$ radii, ω_0 and z_0, in radial and axial direction, respectively, $t_D = \omega_0^2/4D$, the characteristic time for translational diffusion of the observed molecules with the diffusion coefficient, D, through the detection volume, A the average fraction of molecules within a so-called dynamic quenched state, t_A the characteristic correlation time of this quenched state and T the average fraction of molecules in the excited triplet state with a characteristic triplet correlation time, t_T [11].

Fig. 3 shows the measured autocorrelation curves of TMR-EF_1 in the absence of nucleotides and in the presence of AMPPNP together with the weighted residuals [16] of a fit of the data to Eq. 1, indicating a very precise description of the data by Eq. 1. The optical parameter (ω_0/z_0) was determined by fitting the rhodamine 6G FCS data and fixed for all subsequent fits. All other parameters were allowed to vary freely. The FCS data of pure rhodamine 6G and TMR-glutathione (data not shown) could be described properly by an autocorrelation function, $G(t_c)$, just using the diffusion and triplet terms of Eq. 1, i.e. the four parameters, N_F, t_D, T and t_T. In the case of TMR-EF_1 the addition of the so-called dynamic term, i.e. of the parameters A and t_A, is necessary. Obviously, this additional term, with parameters A and t_A, in Eq. 1 is only required for an optimal fit of the TMR-EF_1 data and, therefore, it reflects a property of the fluorophore in the protein environment. Table 1 shows the parameters of the proper fits of the FCS data from measurements of different samples to $G(t_c)$.

From the concentrations, c, of the different solutions and the size of the detection volume, $V = 7.7$ fl (see Section 2), an average number of molecules, $N = c \times V$, in this volume can be calculated: TMR-EF_1 solutions: $N = 0.5$, TMR-glutathione solution: $N = 0.32$, rhodamine 6G solution: $N = 4.6$. These estimations of N are in good agreement with the average

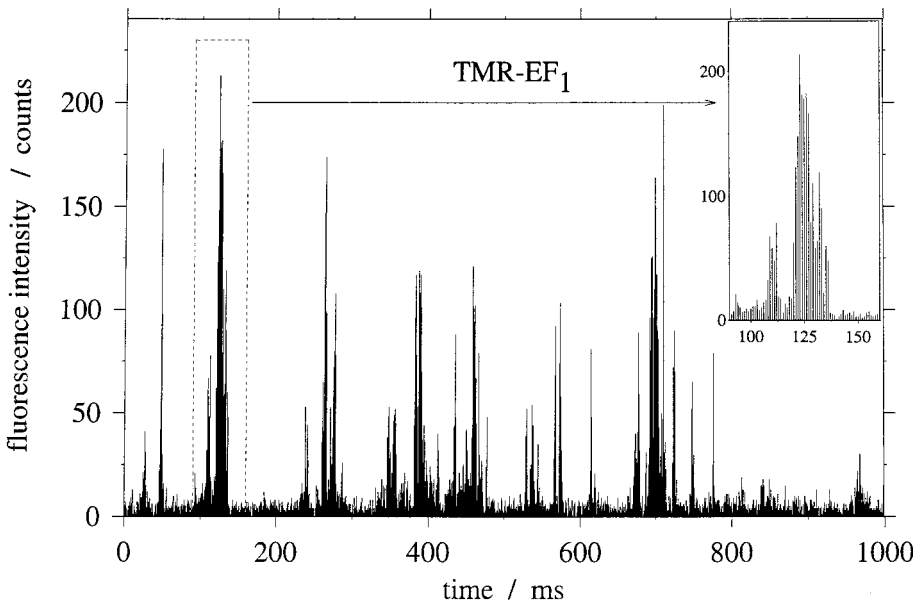

Fig. 3. Normalized fluorescence autocorrelation curves of TMR-EF_1. Solid line: TMR-EF_1 without added nucleotides. Dashed line: TMR-EF_1 in the presence of 1mM AMPPNP normalized to the curve without nucleotides. The weighted residuals [16] from the fit of the data to Eq. 1 are shown at the bottom. Fit parameters are summarized in Table 1.

number of fluorescent molecules, N_F, obtained from FCS (Table 1).

From Table 1 and Fig. 3 it becomes obvious that the addition of nucleotides (ATP or AMPPNP) to TMR-EF_1 results in a significant change of the characteristic diffusion time t_D. After addition of 1 mM ATP, t_D decreased by a factor of 0.81, while addition of 1 mM AMPPNP resulted in a decrease of t_D by a factor of 0.87. The same effects could also be observed in additional experiments where an enlarged confocal detection volume was employed. Using the relation $t_D = \omega_0^2/4D$, between the known radial $1/e^2$ radius, $\omega_0 = 0.65$ μm, and the characteristic translational diffusion time, t_D, the translational diffusion coefficient, D, of TMR-EF_1 can be calculated: $D(\text{TMR-EF}_1) = 3.3 \times 10^{-7}$ cm^2 s^{-1}, addition of 1 mM ATP: $D(\text{TMR-EF}_1, \text{ATP}) = 4.1 \times 10^{-7}$ cm^2 s^{-1}, and addition of 1 mM AMPPNP: $D(\text{TMR-EF}_1, \text{AMPPNP}) = 3.8 \times 10^{-7}$ cm^2 s^{-1}. It is obvious that the addition of the nucleotides increases the diffusion coefficient of TMR-EF_1, and that this effect is more enhanced with ATP.

The diffusion coefficient, D, is related to the frictional coefficient, f, via $D = kT/f$, where k is the Boltzmann constant and T the absolute temperature. At constant temperature and viscosity, the frictional coefficient, f, depends on the radius and the shape of the molecule [17]. We therefore conclude that binding of nucleotides (either ATP or AMPPNP) leads to a large conformational change in the F_1 part of the enzyme.

Similar large conformational changes in the F_1 part of H^+-ATPases were observed with completely different methods. Treatment of mitochondrial MF_1 with glycerol resulted in a release of the bound nucleotides and in a large decrease of the sedimentation coefficient, s, (from 11.9 S to 8.4 S) [18]. This large change was reversed when glycerol was removed.

Direct evidence for a large change of shape upon nucleotide binding comes from X-ray analysis. The X-ray structure of mitochondrial F_1 with the subunits $\alpha_3\beta_3\gamma\delta\varepsilon$ containing three AMPPNP, one ADP, and one ATP per enzyme has been determined [19]. Recently, the X-ray structure of the subcomplex $\alpha_3\beta_3$ from the bacillus PS 3 containing no bound nucleotides has been determined as well [20]. Although the molecular masses of the subunits α and β of PS 3 are similar to that of mitochondrial F_1 and the $\alpha_3\beta_3$ complex does not contain the γ-, δ-, and ε-subunits, it is much larger than the mitochondrial F_1. The main difference between the two structures seems to be that all three nucleotide binding pockets on the β-subunits are empty and in the open conformation in $\alpha_3\beta_3$, whereas in MF_1 only one β-subunit is in such a conformation. Presumably, the large difference between the two structures resulted at least partly from the different nucleotide occupancy of both enzymes. Supporting this conclusion, small-angle X-ray scattering data indicated a structural change of F_1 from PS 3 upon ADP binding which was modelled as a shrinkage of the six major subunits by 6% along their major axis [21].

Best fits to the FCS data of TMR labeled EF_1-ATPases were achieved only after introduction of a second bunching term (so-called dynamic quenched term). This term characterizes an equilibrium in the microsecond time range, which influences the fluorescence of the fluorophore. Most interestingly, addition of ATP or AMPPNP affected the 'dynamic' time, t_A, of TMR-EF_1 in opposite directions. With ATP the 'dynamic' time is shortened, indicating an acceleration of this process with respect to TMR-EF_1 without bound ATP. In contrast, with bound AMPPNP the 'dynamic' time is prolonged. Due to the small amplitudes of this effect, the quantification of these processes is currently difficult. However, it might be of special interest since AMPPNP binds tightly to the enzyme but, in contrast to ATP, is not hydrolyzed. Therefore, this 'dynamic' process might be associated with movements of the γ-subunit during catalysis.

The data in Table 1 show longer triplet correlation times and larger amplitudes of TMR-EF_1 compared to TMR-glutathione. This might be an indication that diffusion of oxygen to quench the triplet state of TMR is sterically hindered when the fluorophore is attached to the protein. These data indicate that single molecule fluorescence – either combined with polarized excitation and emission [22] or combined with fluorescence correlation spectroscopy analysis – can provide new information on conformational changes of the F_1 part upon nucleotide binding.

Acknowledgements: We thank Roderick A. Capaldi and Robert Aggeler for generous support and gift of the mutants making this work possible.

References

[1] Pedersen, P.C. and Carafoli, E. (1987) Trends Biochem. Sci. 12, 146–150.
[2] Boyer, P.D. (1997) Annu. Rev. Biochem. 66, 717–749.
[3] Keller, R.A., Ambrose, W.P., Goodwin, P.M., Jett, J.H., Martin, J.C. and Wu, M. (1996) Appl. Spectrosc. 50, 12A–32A.
[4] Börsch, M., Turina, P., Eggeling, C., Fries, J.R., Seidel, C.A.M., Labahn, A. and Gräber, P. (1998) Ital. Biochem. Soc. Trans. 11.
[5] Aggeler, J.A. and Capaldi, R.A. (1992) J. Biol. Chem. 267, 21355–21359.
[6] Gogol, E.J., Luecken, U., Bork, T. and Capaldi, R.A. (1989) Biochemistry 28, 4709–4716.
[7] Turina, P. and Capaldi, R.A. (1994) J. Biol. Chem. 269, 13465–13471.
[8] Gill, S.C. and von Hippel, P.H. (1989) Anal. Biochem. 182, 319–326.
[9] Zander, C., Sauer, M., Drexhage, K.H., Ko, D.-S., Schulz, A., Wolfrum, J., Brand, L., Eggeling, C. and Seidel, C.A.M. (1996) Appl. Phys. B 63, 517–523.
[10] Brand, L., Eggeling, C., Zander, C., Drexhage, K.H. and Seidel, C.A.M. (1997) J. Phys. Chem. A. 101, 4313–4321.
[11] Widengren, J., Mets, Ü. and Rigler, R. (1995) J. Phys. Chem. 99, 13368–13379.
[12] Elson, E.L. and Magde, D. (1974) Biopolymers 13, 1–27.
[13] Thompson, N.L. (1991) in: Topics in Fluorescence Spectroscopy, Volume 1: Techniques (Lakowicz, J.R., Ed.), pp. 337–378, Plenum Press, New York.
[14] Eggeling, C., Widengren, J., Rigler, R. and Seidel, C.A.M. (1998) Anal. Chem. 70, 2651–2659.
[15] Fries, J.R., Brand, L., Eggeling, C., Köllner, M. and Seidel, C.A.M. (1998) J. Phys. Chem. A (in press).
[16] Koppel, D.E. (1974) Phys. Rev. A 10, 1938–1946.
[17] Tanford, C. (1961) Physical Chemistry of Macromolecules, Wiley, Chichester.
[18] Garret, N.E. and Penefsky, H.S. (1975) J. Supramol. Struct. 3, 469–478.
[19] Abrahams, J.P., Leslie, A.G.W., Lutter, R. and Walker, J.E. (1994) Nature 370, 621–628.
[20] Shirakihara, Y., Leslie, A.G.W., Abrahams, J.P., Walker, J.E., Ueda, T., Sekimoto, Y., Kambara, M., Saika, K., Kagawa, Y. and Yoshida, M. (1997) Structure 5, 825–836.
[21] Furuno, T., Ikegami, A., Kihara, H., Yoshida, M. and Kagawa, Y. (1983) J. Mol. Biol. 170, 137–153.
[22] Häsler, K., Engelbrecht, S. and Junge, W. (1998) FEBS Lett. 426, 301–304.